hnRNP A2 Selectively Binds the Cytoplasmic Transport Sequence of Myelin Basic Protein mRNA†

Keith S. Hoek,‡ Grahame J. Kidd,‡ John H. Carson,§ and Ross Smith*,‡

Department of Biochemistry, University of Queensland, Queensland 4072, Australia, and Department of Biochemistry, University of Connecticut Health Center, Farmington, Connecticut 06030

Received January 5, 1998; Revised Manuscript Received February 16, 1998

ABSTRACT: Segregation of mRNAs in the cytoplasm of polar cells has been demonstrated for proteins involved in *Xenopus* and *Drosophila* oogenesis, and for some proteins in somatic cells. It is assumed that vectorial transport of the messages is generally responsible for this localization. The mRNA encoding the basic protein of central nervous system myelin is selectively transported to the distal ends of the processes of oligodendrocytes, where it is anchored to the myelin membrane and translated. This transport is dependent on a 21-nucleotide *cis*-acting segment of the 3′-untranslated region (RTS). Proteins that bind to this *cis*-acting segment have now been isolated from extracts of rat brain. A group of six 35−42-kDa proteins bind to a 35-base oligoribonucleotide incorporating the RTS, but not to several oligoribonucleotides with the same composition but randomized sequences, thus establishing specificity for the base sequence in the RTS. The most abundant of these proteins has been identified, by Edman sequencing of tryptic peptides and mass spectroscopy, as heterogeneous nuclear ribonucleoprotein (hnRNP) A2, a 36-kDa member of a family of proteins that are primarily, but not solely, intranuclear. This protein was most abundant in samples from rat brain and testis, with lower amounts in other tissues. It was separated from the other polypeptides by using reverse-phase HPLC and shown to retain preferential association with the RTS. In cultured oligodendrocytes, hnRNP A2 was demonstrated by confocal microscopy to be distributed throughout the nucleus, cell soma, and processes.

Differentiation of many cells is accompanied by the development of structural and functional asymmetry. Vectorial transport of mRNAs and localized translation provides one means for establishing the polarized distribution of proteins in these cells. In oogenesis and embryonic development, for example, mRNAs encoding many essential morphogenic proteins are selectively targeted to different subcellular domains, including those encoding *oskar*, *nanos*, and *bicoid* in *Drosophila* and *Vg1* and *Xcat*-2 in *Xenopus* (*1, 2*). Mislocalization of these mRNAs results in aberrant embryogenesis. In somatic cells, mRNAs encoding some key intracellular proteins are also concentrated in discrete locations. Examples include the RNAs encoding important structural proteins such as β-actin, which is concentrated at the leading edge of fibroblasts (*3*), MAP2 and tau, which are asymmetrically distributed in neurons (*4, 5*), and myelin basic protein (MBP) mRNAs, which accumulate at the myelinating periphery of oligodendrocytes (*6, 7*). MBP mRNA transport was one of the first recognized examples (*6*), and it remains one of the better characterized.

Central nervous system myelin is a morphologically complex, spiralled extension of the oligodendrocyte plasma membrane which ensheaths axonal processes. Subcellular fractionation and immunostaining studies have shown that MBP, a major structural component, is concentrated in compact myelin membrane (*8*−*10*). Studies of mice expressing MBP mutations (e.g., *Shiverer*) indicate that this protein is involved in the close association between cytoplasmic surfaces at the dense line of myelin lamellae (*10, 11*) and is essential for central nervous system myelination. This localization of MBP appears to be effected primarily by segregation of its message to the myelinating periphery of oligodendrocytes, followed by protein synthesis and incorporation into compact myelin (*6, 12*). Initially, mRNAs encoding MBP are concentrated near oligodendrocyte nuclei, but they redistribute to the myelin sheath at the onset of myelination (*7, 13*). While mRNAs for the tau isoforms are also peripherally translocated in vivo (*14*), others, such as that encoding the myelin proteolipid protein, are restricted to the cell body (*7, 13*), indicating that peripherally directed mRNA transport is a selective event.

Active, multistep MBP message transport has been described in cultured oligodendrocytes. Exogenous MBP transcripts microinjected into the oligodendrocyte soma collect into granules and move from the cell body into the myelin-forming processes (*15, 16*). These granules also contain arginyl-tRNA synthetase, elongation factor 1α, and ribosomal RNA, which suggests that they carry all of the machinery necessary for translation of mRNA at the periphery (*17*). Deletion experiments conducted with MBP mRNA have established that a *cis*-acting sequence which is necessary

† This work was supported by grants from the Australian National Health and Medical Research Council and the National Multiple Sclerosis Society of Australia to R.S. and G.J.K.

* Corresponding author. Telephone: 61 7 3365 4627. Facsimile: 61 7 3365 4699. E-mail: ross@biosci.uq.edu.au.

‡ University of Queensland.

§ University of Connecticut Health Center.

S0006-2960(98)00024-5 CCC: $15.00
Published on Web 04/22/1998

and sufficient for RNA transport, the RNA transport sequence (RTS),[1] lies within a 21-nt stretch of the 3′-untranslated region (UTR) (*18*).

To identify *trans*-acting factors involved in the transport of MBP mRNA, we have employed a binding assay using a 35-nt RNA containing the RTS. We describe the isolation of a group of six proteins that bind the RTS in a sequence-dependent manner. The dominant binding protein has been identified as a member of the family of heterogeneous nuclear ribonucleoproteins, hnRNP A2. Immunostaining using a highly specific chicken antibody indicated that hnRNP A2 not only is located in the nucleus of oligodendrocytes but also is abundant in granules found in the cell body and processes.

MATERIALS AND METHODS

Biotinylated Oligonucleotides. RNAs 35 nt in length were synthesized by Oligos Etc., Inc. (Wilsonville, OR). The purity of these oligoribonucleotides was confirmed by electrophoresis on both agarose and polyacrylamide gels of aliquots of equal 260-nm absorbance. Dot-blot analysis of serially diluted aliquots with alkaline phosphatase-linked streptavidin demonstrated that efficiency of biotinylation was the same for all probes.

Protein Extraction. Tissues were removed from 21-day-old Wistar rats and placed in ice-cold phosphate-buffered saline (PBS) immediately prior to homogenization. Extranuclear and nuclear protein extracts were prepared as described (*19*). High-salt protein extracts ("cytoskeletal fractions") were then obtained using the following method. The pellet remaining after extranuclear/nuclear extraction was resuspended by vortexing in 1 vol of extract buffer (20 mM HEPES, 0.65 M KCl, 2 mM EGTA, 1 mM $MgCl_2$, 2 M glycerol, 14.3 mM β-mercaptoethanol, 8.7 mM Nonidet-P40, 12.1 mM deoxycholic acid, 1 mM PMSF, and 21 μM leupeptin, pH 7.4). This was centrifuged at 13000*g* for 15 min at 4 °C; the supernatant (cytoskeletal fraction) was removed and kept at 4 °C. Protein concentrations in the extract fractions were estimated colorimetrically using the Bio-Rad protein assay reagent (Bio-Rad, Hercules, CA). Where binding assays required unfractionated tissue extracts, tissues were homogenized in the above extract buffer and centrifuged at 13000*g* for 15 min at 4 °C.

Affinity Isolation of RNA-Binding Proteins. Streptavidin-coated superparamagnetic particles and magnetic particle separators were purchased from Boehringer Mannheim GmbH (Mannheim, Germany). For each RNA-binding assay 0.5 mg of magnetic particles was incubated on ice for 10 min with 2 μg of biotinylated 35-nt RNA in a 250-μL solution of 10 mM Tris-HCl, 1 mM EDTA, and 100 mM NaCl, pH 7.5. Unbound RNA was washed off with 10 mM Tris-HCl, 1 mM EDTA, and 1 M NaCl, pH 7.5. In a standard 1-mL assay about 5 mg of brain protein was added to 0.5 mg of the RNA-labeled magnetic particles, which had a theoretical capacity of 0.1 nmol of RTS. Binding took place for 30 min on ice in binding buffer (10 mM HEPES, 3 mM $MgCl_2$, 40 mM NaCl, and 5% glycerol, pH 7.5) and 10 g/L heparin to reduce nonspecific binding. Then the particles were concentrated magnetically, and the supernatant was aspirated. The particles were washed three times with binding buffer before protein bound to the particles was released by incubation in 50 μL of 0.1% SDS and 1 mM DTT and heating to 65 °C for 10 min. After removal of the magnetic particles, the protein solution was brought to 4% sodium dodecyl sulfate (SDS), 10% sucrose, 0.5% β-mercaptoethanol, and 0.01% bromophenol blue by the addition of concentrated electrophoresis sample buffer, heated to 65 °C for 10 min, and electrophoresed on a 12% polyacrylamide gel containing SDS. After electrophoresis, gels were stained with B/T Blu*v* protein stain (B/T Scientific Technologies, Carlsbad, CA).

Several nonspecific RNAs were used as controls, and unlabeled, streptavidin-coated particles were also used as controls for nonspecific binding. In competition RNA-binding assays, RTS RNA-labeled particles and RNA competitor (25-fold excess of unbiotinylated RTS or NS1 RNA) were co-incubated with 5 mg of brain protein in binding buffer. For preparative isolation of RNA-binding proteins, 5 mg of RTS RNA-labeled streptavidin-coated particles were incubated with 50 mg of brain cytoskeletal fraction in 10 mL using the standard assay conditions above.

Reverse-Phase HPLC of RTS-Binding Proteins. Protein was released from streptavidin-coated particles by incubation in 30% acetonitrile and 0.1% TFA at 65 °C for 10 min. This solution was diluted to 5% acetonitrile by addition of 0.1% TFA before it was passed through a 0.2-μm filter and loaded onto a 5 × 0.46 cm diam Poros HR 10 reverse-phase HPLC column (PerSeptive Biosystems Inc., Framingham, MA) which had been equilibrated with 5% acetonitrile in 0.1% TFA at 20 °C. The column was washed with 2.5 mL of the same solvent, followed by a 4-min linear gradient to 90% acetonitrile in 0.1% TFA. The same procedure was followed for larger-scale isolation of the RTS-binding proteins except that the initial solvent contained 25% acetonitrile and was followed by a 6-min linear gradient to 55% acetonitrile. Elution was monitored by measuring the absorbances at 280 and 214 nm.

Mass Spectroscopy. The mass of HPLC-purified rat hnRNP A2 was measured by mass spectrometry (MS) on a single-quadrupole mass spectrometer fitted with an electrospray ion source (API165, PE-SCIEX Instruments, Toronto, ON, Canada). Samples were injected at 10 μL/min into the solvent delivery line of the spectrometer operated in the positive ion mode (electrospray voltage, +4.5 kV; orifice potential, 80 V). Scan conditions were *m*/*z* 1200 to 2400 in 5 s with a step of 0.5 atomic mass units. Spectra were collected using multichannel averaging.

RTS-Binding Analyses of HPLC-Purified Proteins. Proteins purified by reverse-phase HPLC were removed from acetonitrile and TFA by centrifugation over 10-kDa cutoff filters (Millipore, Sydney, Australia) and taken up in binding buffer. RTS-binding analyses were carried out as described above for affinity purification studies, except that 5 mg/mL BSA was included to inhibit nonspecific protein binding to the surface of the magnetic particles. RTS-binding samples

[1] Abbreviations: DMEM, Dulbecco's modified Eagle medium; DTT, dithiothreitol; HEPES, *N*-(2-hydroxyethyl)piperazine-*N*′-2-ethanesulfonic acid; hnRNP, heterogeneous nuclear ribonucleoprotein; MBP, myelin basic protein; NS, nonspecific RNA; nt, nucleotide; PMSF, phenylmethanesulfonyl fluoride; PVDF, polyvinylidine difluoride; RTS, MBP mRNA transport sequence; RAP, RTS-associated polypeptide; SDS, sodium dodecyl sulfate; TFA, trifluoroacetic acid; UTR, untranslated region.

were analyzed by SDS-polyacrylamide electrophoresis as described above.

Protein Sequencing. Samples containing protein taken from a preparative-scale RNA-binding experiment were electrophoresed under reducing conditions on a 12% polyacrylamide gel containing SDS. After electrophoresis, the gel was lightly stained with B/T Blu*v* blue protein stain and the band of interest was excised from the gel. The gel slice was pulverized in a microfuge tube, and 200 μL of 100 mM sodium phosphate buffer, pH 8.0, containing 10 μg of trypsin (Sigma Chemical Co., St. Louis, MO) was added. This was incubated at 37 °C overnight and then centrifuged at 13000*g* for 30 min at room temperature. The supernatant was removed and placed in a microfuge tube, and the pellet was washed with 200 μL of water and recentrifuged. Pooled supernatants were acidified to 0.1% TFA and centrifuged at 13000*g* for 30 min at room temperature. Reverse-phase HPLC was used to purify tryptic fragments before N-terminal sequencing. A 25 × 0.46 cm i.d. analytical column (Alltech C8, 5 μm silica bead matrix) was equilibrated with 5% solvent acetonitrile and 0.1% TFA at 1 mL/min and 25 °C. After sample loading, the column was then subjected to a 40-min linear gradient of 5−40% acetonitrile and 0.1% TFA in 0.1% aqueous TFA, followed by a 20-min linear gradient to 80% acetonitrile and 0.1% TFA. Eluate from the column was monitored at 280 and 214 nm. Fractions of sufficient homogeneity were concentrated by lyophilization, applied to polybrene-treated glass-fiber filters, and subjected to N-terminal Edman sequencing on an Applied Biosystems (Foster City, CA) 470A protein sequencer with an on-line PTH analyzer. Sequences obtained were used to query the ATLAS sequence retrieval program, located at the Martinsried Institute for Protein Sequences, accessing the PIR, SWISSPROT, GB, and EMBL protein sequence databases.

Immunoblotting. Samples resolved by SDS−polyacrylamide gel electrophoresis were transferred from gel to Immobilon polyvinylidine difluoride membrane (Millipore, Sydney, Australia) by electroblotting in 10 mM 3-[cyclohexylamino]-1-propanesulfonate, pH 11. The filter was blocked with a solution of 5% skim milk and 0.02% Tween 20 in PBS. The filter was incubated with 7A9 monoclonal antibody (*20*), at 1:3000 dilution, for 1.5 h in 1:10 blocking solution in PBS and washed three times with 0.02% Tween 20 in PBS and then once in Tris-buffered saline (TBS). Alkaline phosphatase-conjugated sheep anti-mouse IgG (Silenius Laboratories, Hawthorn, Australia) diluted 1:2000 in the antibody incubation solution was added to the filter for 1.5 h. After three washes with TBS, antigen−antibody complexes were visualized by reaction with a freshly prepared solution of 0.1 M Tris-HCl (pH 9.5), 150 mM NaCl, and 50 mM $MgCl_2$ containing 0.48 mM nitroblue tetrazolium and 0.56 mM 5-bromo-4-chloro-3-indolyl phosphate.

Immunostaining of Oligodendrocytes and COS-1 Cells. Oligodendrocyte-enriched cultures were generated from newborn rat and mouse brains as previously described (*15*, *17*). Oligodendrocytes were plated onto coverslips and allowed to differentiate for 2−3 days prior to treatment. The cells were fixed for 30 min at room temperature with 4% paraformaldehyde in phosphate-buffered saline (PBS) that contained 5 mM $MgCl_2$.

COS-1 cells were grown in DMEM containing 10% fetal calf serum and fixed as above.

Since the 7A9 antibody recognizes multiple hnRNPs (*20*), these experiments used a chicken antibody, HK334-8, which had been fractionated by ion-exchange chromatography to concentrate hnRNP A2-specific antibodies (A. Hawkins et al., unpublished observations). After permeabilization in 0.1% NP40 detergent in PBS for 4.5 min, the fixed oligodendrocytes or COS-1 cells were washed in PBS and then blocked in 5% normal goat serum diluted in PBS. The HK334-8 antibody was diluted 1:50 in the blocking solution, and cells were incubated in this reagent for 30 min at room temperature. After repeated PBS washings, the coverslips were blocked again and then incubated in 1:50 fluorescein isothiocyanate-conjugated antibodies directed against chicken immunoglobulins (Promega and Sigma-Aldrich, Sydney, Australia). In double-labeling experiments, cells were subsequently stained using a mouse monoclonal antibody against myelin basic protein (Sternberger Meyer, MD) followed by tetramethyl rhodamine isothiocyanate-conjugated secondary antibodies (Sigma-Aldrich). After washes in PBS, cells were mounted in glycerol containing 3% 1,4-diazabicyclo[2.2.2.]octane as an antibleaching agent. The cells were viewed on a Zeiss Axiophot 2 fluorescence microscope and imaged with a Variophot CCD camera. Confocal microscopy was undertaken using Zeiss and Bio-Rad instruments equipped with ×40 (1.25 NA) and ×63 (1.4 NA) lenses. Control experiments in which primary and/or secondary antibodies were withheld resulted in no significant fluorescence.

RESULTS

A Small Group of Proteins Binds the RTS Selectively. Rat brain fractions were added to streptavidin-coated magnetic particles bearing a biotinylated 35-nt oligoribonucleotide incorporating the RTS sequence. After washing, bound proteins were recovered from the particles by elution with SDS/DTT and analyzed by SDS gel electrophoresis, or they were eluted with 30% acetonitrile in 0.1% TFA and analyzed by reverse-phase HPLC. Many proteins were bound to the streptavidin-coated particles in the absence of RNA, but these nonspecific interactions were largely suppressed by the inclusion of 10 g/L heparin in the binding assays. A group of six proteins with apparent molecular masses between 35 and 42 kDa were consistently eluted from the RTS-labeled magnetic particles, usually accompanied by a small number of polypeptides that also were bound to particles without attached RNA. Figure 1A shows a typical SDS gel profile for the bound proteins, which are dominated by a single 36-kDa polypeptide. Addition of fresh RTS-bearing magnetic particles to brain protein extract already used in one experiment resulted in the isolation of little more of the RNA-binding proteins, and there consequently appears to be only a few micrograms of these proteins in 5 mg of brain protein. Reverse-phase HPLC on the Poros column resolved the RNA-binding proteins into two peaks distinct from those arising from nonspecifically bound proteins (Figure 1B). The slower component (B) gave a single band at 36 kDa on subsequent SDS gel electrophoresis, while the faster (A) contained all five of the remaining RTS-associated polypeptides (RAPs) (Figure 1B, inset).

To distinguish proteins that bind the RTS in a sequence-dependent manner from those that bind nonspecifically to RNA, the binding experiments were repeated with an

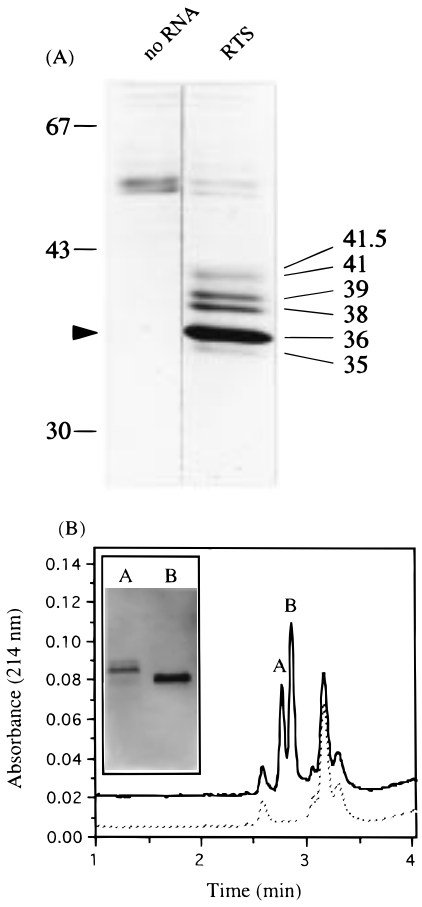

FIGURE 1: RTS-binding proteins of rat brain. (A) Proteins were isolated from a rat brain cytoskeletal fraction by RNA-free (left lane) or RTS-linked (right lane) magnetic particles, electrophoresed on SDS−polyacrylamide gels, and stained with B/T Bl*v*. From its mobility, the major RTS-binding polypeptide (arrowhead) has an apparent molecular mass of 36 kDa. The positions of standard proteins and their molecular masses, in kilodaltons, are shown at left. This pattern of RTS-binding proteins is highly reproducible, but the resolution and visibility of the minor polypeptides is dependent on the amount of protein loaded and the distance over which the proteins are run, leading to variability in the appearance of these bands in some of the later figures. (B) Reverse-phase HPLC of RTS-binding proteins. Rat brain proteins eluted from RTS-labeled magnetic particles by incubation in 30% acetonitrile and 0.1% TFA were filtered and diluted to 5% acetonitrile and 0.1% TFA before injection onto a Poros HR 10 reverse-phase HPLC column (5 × 0.46 cm). The proteins were eluted with a gradient of 5% to 90% acetonitrile and 0.1% TFA over 4 min at a flow rate of 5 mL/min. The 214-nm elution pattern of proteins isolated from RTS RNA-labeled magnetic particles is indicated by the solid line, and that of proteins isolated from unlabeled particles (control) is indicated by the dashed line. Inset: SDS gel electrophoresis of RTS-binding proteins separated by HPLC. Peak A contains the RTS-associated polypeptides (RAPs, 35−41 kDa), and peak B, the 36-kDa hnRNP A2.

additional three oligoribonucleotides having the same base composition as the RTS-containing molecule, but with randomly rearranged sequences (Figure 2A). A fifth 35-mer with a sequence matching part of the 5′-untranslated region of the MBP mRNA was also used. To gauge the relative affinities of these RNAs for the proteins, the amount of protein added was less than that required to saturate the binding capacity of the RTS-bearing particles. Under these conditions, the association of the 36-kDa protein with the randomized oligonucleotides was negligible (Figure 2B) and the minor proteins were not detected (Figure 2C). Analysis

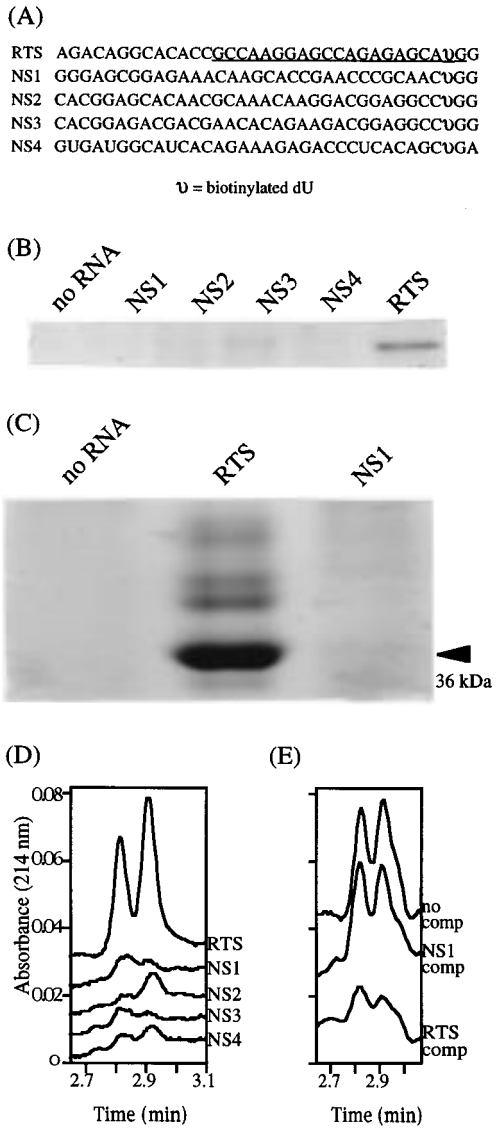

FIGURE 2: Specificity of the RNA−protein interactions. (A) The biotinylated sequences of the RNA transport segment (RTS) and the four nonspecific RNAs (NS1−NS4). NS 1−3 are identical in nucleotide composition to the RTS, but their sequences are randomized, except for the three 3′-nucleotides. NS4 is homologous to a sequence within the 5′-untranslated region of rat MBP mRNA. The 21-nt RTS sequence, which was more closely defined during the course of this work (*18*), is underlined in the 35-nt sequence at the top. For simplicity, we have retained the designation RTS to identify the larger oligoribonucleotide. (B) Comparison of the retention of the 36-kDa polypeptide on particles bearing specific and nonspecific (NS) RNAs. The SDS−polyacrylamide gel was stained with B/T Bl*v* protein stain. In this experiment the amount of added tissue protein was reduced to ensure that the binding capacity of the RTS-bearing particles was not saturated; under these conditions the minor polypeptides are not detected. The amounts of RNA and magnetic particles were constant. (C) By using saturating amounts of protein, the minor RTS-binding polypeptides were also detectable by SDS−PAGE and B/T Bl*v* stain in eluates from RTS-bearing particles, but not those carrying the nonspecific RNA. (D) RTS-binding proteins specific for RTS RNA. Protein extracts of rat brain were incubated with magnetic particles bearing the RTS or the other nonspecific probes, and the eluted proteins were analyzed by HPLC. (E) RTS-labeled particles exposed to rat brain protein extracts in the presence or absence of excess RNA competitors. The 36-kDa RTS-binding protein is largely competed away by a 25-fold excess of RTS RNA (RTS comp), but not by an excess of NS1 nonspecific RNA (NS1 comp).

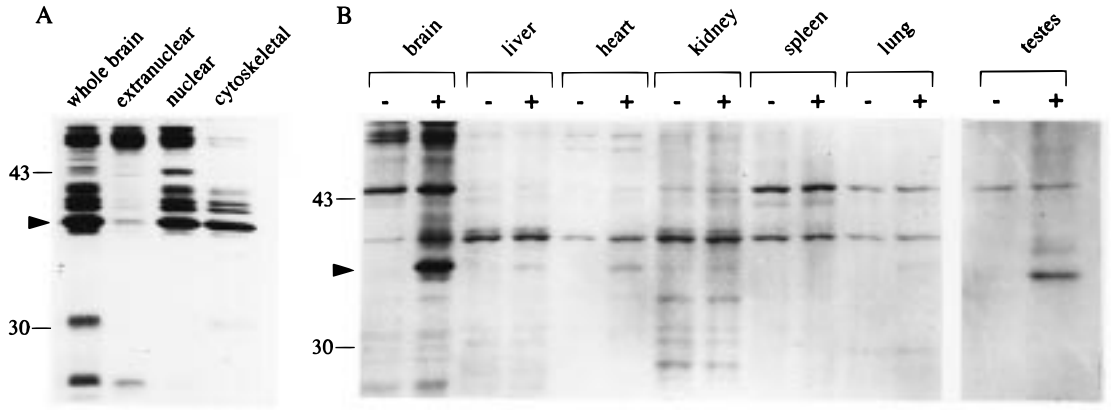

FIGURE 3: Subcellular and tissue distribution of RTS-binding proteins. (A) Subcellular protein extracts of rat brain were incubated with RTS-labeled magnetic particles, and the bound proteins were eluted and analyzed on SDS−polyacrylamide gels. The 36-kDa RTS-binding protein (arrowhead) is present in nucleoplasmic and cytoskeletal extracts, but it is low in the cytosolic (extranuclear) fraction. The minor RTS-associated proteins are visible in these assays. (B) Total tissue extracts were incubated either with unlabeled magnetic particles (−) or with RTS-labeled (+) particles. Equal amounts of tissue protein were used in each RTS-binding experiment. The 36-kDa RTS-binding protein (arrowhead) is clearly present in brain and testis, and it is weakly detected in liver, heart, and lung.

by HPLC of the proteins bound to magnetic particles, which provides a more quantitative comparison of the protein binding to the RNAs, again demonstrated specific binding to the RTS (Figure 2D).

In competition assays, co-incubation with a 25-fold excess of a nonspecific RNA, NS1, weakly interfered with the RTS binding of the 36-kDa protein, but addition of excess RTS RNA to the extracts markedly reduced the amount of this protein recovered from the RTS-labeled particles, confirming the specificity of its interaction with the RTS-containing RNA (Figure 2E).

The 36-kDa RTS-binding protein was present in nuclear extracts (Figure 3A), but a significant amount was also recovered from cytoskeletal (i.e., high salt, detergent) fractions. It was barely detectable in cytoplasmic (low salt, no detergent) fractions. Binding experiments performed with total cell proteins extracted from a variety of rat tissues showed the highest levels of this protein in brain and testis, with small amounts in liver and heart, and the lowest levels were in kidney, spleen, and lung (Figure 3B).

The 36-kDa Protein Is a Heterogeneous Nuclear Ribonucleoprotein. The 36-kDa protein was obtained by repeating the analytical binding experiment on a 10-fold larger scale. The SDS gel bearing the RTS-binding proteins was electroblotted onto polyvinylidine difluoride (PVDF) membrane, the proteins were lightly stained, and the appropriate band was cut out. Attempts to sequence the intact protein were unsuccessful, suggesting that the amino-terminus was blocked. To generate peptide fragments, the blotted protein was cleaved with trypsin, and the peptides were eluted from the PVDF before separation by reverse-phase HPLC. Several purified peptides were subjected to automated Edman sequencing, yielding the sequences depicted in Figure 4. Computer searches of the PIR, SWISSPROT, GB, and EMBL protein sequence databases revealed complete identity of the 59 sequenced residues with those of two closely related members of the family of heterogeneous nuclear ribonucleoproteins, human hnRNPs A2 and B1.

The identification as an hnRNP was confirmed by Western blotting with the 7A9 monoclonal antibody, which reacts with A2/B1 and also recognizes other A, B, G, E, H, and L hnRNPs (*21*). Immunostaining of RTS-binding proteins

```
1    MEREKEQFRKLFIGGLSFETTEESLRNYYEQWGKLTDCVVMRDPASKRSR   50
51   GFGFVTFSSMAEVDAAMAARPHSIDGRVVEPKRAVAREESGKPGAHVTVK  100
101  KLFVGGIKEDTEEHHLRDYFEEYGKIDTIEIITDRQSGKKRGFGFVTFDD  150
151  HDPVDKIVLQKYHTINGHNAEVRKALSRQEMQEVQSSRSGRGGNFGFGDS  200
201  RGGGGNFGPGPGSNFRGGSDGYGSGRGFGDGYNGYGGGPGGGNFGGSPGY  250
251  GGGRGGYGGGGPGYGNQGGGYGGGYDNYGGGNYGSGNYNDFGNYNQQPSN  300
301  YGPMKSGNFGGSRNMGGPYGGGNYGPGGSGGSGGYGGRSRY           341
```

FIGURE 4: Microsequencing of the 36-kDa RTS RNA-binding protein. The rat 36-kDa RTS-binding protein was digested with trypsin and fractionated by reverse-phase HPLC, yielding several isolated peptide fragments that were subjected to Edman sequencing. The sequences obtained were used to interrogate protein sequence databases. All fragments showed 100% identity to human hnRNP A2/B1. The sequence of human hnRNP A2 (*22*) is shown; underlined regions represent sequences obtained in this study.

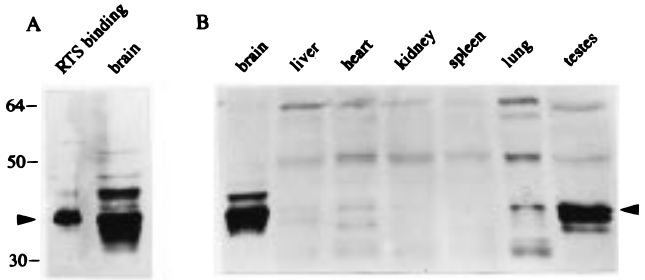

FIGURE 5: Western blot analyses of hnRNP A2/B1 in total cell proteins from various tissues. (A) Immunostaining of RTS-binding proteins compared to whole rat brain extract, using 7A9 antibody. The 36-kDa hnRNP A2 (arrowhead) is the predominant 7A9-positive RTS-binding protein in rat brain. (B) Tissue distribution analysis shows that it is also present at high concentrations in testis and at lower levels in liver, heart, and lung.

revealed a major band at 36 kDa and a less prominent band at 41 kDa (Figure 5A). To investigate whether the hnRNPs that bound to the RTS were representative of the hnRNP A and B content of rat brain, extracts containing combined nucleoplasmic, cytoplasmic, and cytoskeletal fractions were Western blotted and the pattern of 7A9-positive bands was compared with those of the RTS-binding polypeptides (Figure 3B). In rat brain, prominent bands were observed at ~34 and ~36 kDa (Figure 5A). The upper of these two bands comigrated with recombinant human hnRNP A2 (not shown) and with the 36-kDa RTS-binding protein. From

its abundance, 7A9 immunoreactivity, and relative electrophoretic mobility, the lower band appeared to be hnRNP A1. hnRNP A2 was the most prominent RTS-binding protein, with little or no hnRNP A1 bound to the MBP mRNA-derived sequence.

Human hnRNPs A2 and B1 differ by the inclusion of an additional 11 amino acid sequence near the amino-terminus in B1 (*22*). Is the 36-kDa protein A2 or B1? The full sequences of the rat A2/B1 proteins are unknown; however, there appears to a high level of sequence identity between the rat and human proteins: the published human and rat hnRNP A1 sequences differ in a single residue (*23, 24*), and the 65% of the cDNA sequence we have obtained so far for the rat 36-kDa protein (A. Hawkins et al., unpublished results) also shows complete sequence identity with the human A2/B1. Electrospray mass spectroscopy gave a molecular mass of 36 080 ± 10 Da for the purified RTS-binding protein (see below), a value much closer to the calculated mass of 36 007 Da for human A2 than to the 37 430 Da of human B1. Although full sequences for rat A2 and B1 will be required to unambiguously identify the RTS-binding isoform, the above evidence and the pattern obtained on Western blots with an antibody known to interact primarily with hnRNP A2/B1 suggest that it is hnRNP A2.

The RTS-Binding hnRNP Is Concentrated in Rat Brain and Testis. In HeLa cell nuclei, hnRNPs A2 and B1 form core particles of defined stoichiometry with hnRNPs A1, B2, C1, and C2. These particles are thought to form on nascent RNA and carry out such functions as splice regulation and nuclear transport (*25*). If this were the only role for hnRNP A2/B1, a fairly uniform distribution of this protein between tissues could be anticipated. However, in RTS-binding studies, the levels of the 36-kDa hnRNP detected in brain and testis extracts greatly exceeded those in other tissues (Figure 3B).

As hnRNPs can undergo posttranslational modifications which may affect their activities (*26, 27*), it was possible that much of the hnRNP A2 was present in extracts from other tissues in a form unable to bind the RTS. Indeed, previous studies of *nuclear* extracts from rat tissues revealed hnRNP A2 in a variety of other tissues (*28*). To test this possibility, total cell protein extracts were analyzed using Western blots developed with the 7A9 antibody. As shown in Figure 5B, the results paralleled those from the RTS-binding experiments: prominent 36-kDa components were 7A9-positive in brain and testis, with far lower concentrations in other tissues. The presence of such high levels in brain and testis suggests roles in these tissues, in addition to intranuclear functions such as splice site switching and nuclear export.

hnRNP A2 Is Abundant in Oligodendrocytes. While subcellular fractionation indicated that significant pools of hnRNP A2 were attached to the extranuclear cytoskeleton, these experiments did not indicate whether hnRNP A2 was dispersed throughout the cell, as would be expected if it participated in mRNA trafficking and cytoplasmic RNA metabolism. To investigate the cytological distribution of hnRNP A2, rat and mouse oligodendrocytes were grown in tissue cultures until they had elaborated substantial myelin membrane sheets (Figure 6A,B), and then immunostained. The chicken HK334-8 antibody against hnRNP A2 was used, as 7A9 recognizes multiple hnRNP family members (*20*). HK334-8, an ion-exchange-purified chicken antibody that binds isolated rat and human hnRNP A2, revealed only a single major 36-kDa band on Western blots of extracted brain and oligodendrocyte proteins (G. J. Kidd et al., unpublished experiments).

As expected from studies of other cells (*20, 28, 44, 49*), hnRNP A2 antibodies labeled the nuclei of rat and mouse oligodendrocytes and of COS-1 cells (Figure 6). In oligodendrocytes, immunostaining was also abundant in the perinuclear cytoplasm; in many cells (Figure 6C), the intensity of cytoplasmic immunostaining was comparable to that in the nucleus. hnRNP A2 was detected in the major cytoplasmic trunks that radiate peripherally from the cell body and in the fine networks of cytoplasmic channels that extend from these trunks and act as conduits for the transport of vesicles and MBP mRNAs (Figure 6C) (*15*). However, adjacent MBP-rich membrane expanses exhibited only background hnRNP A2 staining. Throughout the oligodendrocyte cytoplasm, the immunofluorescence signal was not diffuse but appeared granular or punctate (Figure 6C); this was most obvious in small cytoplasmic channels. Similar distributions were observed when the 7A9 antibody was used, although the nuclear staining was more intense because 7A9 antibodies bound other, nuclear-localized hnRNPs. In contrast, COS-1 cells exhibited predominantly nuclear staining with the HK334-8 antibody and, under equivalent conditions, showed no cell-associated fluorescence in the absence of the primary antibody (Figure 6D−G).

Binding of Purified hnRNP to the RTS RNA. To determine whether hnRNP A2 could associate with the RTS in the absence of the other, less-abundant polypeptides, it was purified by HPLC after elution from RTS-bearing magnetic particles. Equal amounts of hnRNP A2 were added to particles bearing the RTS and a nonspecific RNA for the isolated protein. Figure 7A shows that the purified protein retains its ability to discriminate between the RTS and another unrelated RNA sequence and that this binding can take place in the absence of the RAPs. In contrast, the RAPs do not bind to the RTS in the absence of hnRNP A2, but do so in its presence (Figure 7B), suggesting either that the former interact with the latter rather than directly with the RTS or that the interaction of the RAPs with the hnRNP A2 leads to allosteric changes that enhance the RTS−RAPs interaction.

DISCUSSION

cis-Acting Sequence for MBP mRNA Transport. There is abundant evidence for the involvement of the noncoding RNA regions in the transport, localization, translation, and stability of many mRNAs (*1, 5, 29*−*33*). Many of these *cis*-acting regions are in the 3′-UTR and may be large and complex (*34*) or small structural elements (*33, 35*).

The role of *cis*-acting sequences in transport of MBP mRNA is comparatively well understood. The element necessary and sufficient for transport to the periphery of oligodendrocyte processes is a 21-nt section of the 3′-UTR (*18*). MBP message injected into the soma of cultured oligodendrocytes is incorporated into granules about 1.4 μm in diameter which move out along the processes, possibly by kinesin-mediated transport along microtubules (*36*), to the sites where myelin is elaborated (*15, 17, 18*). In addition

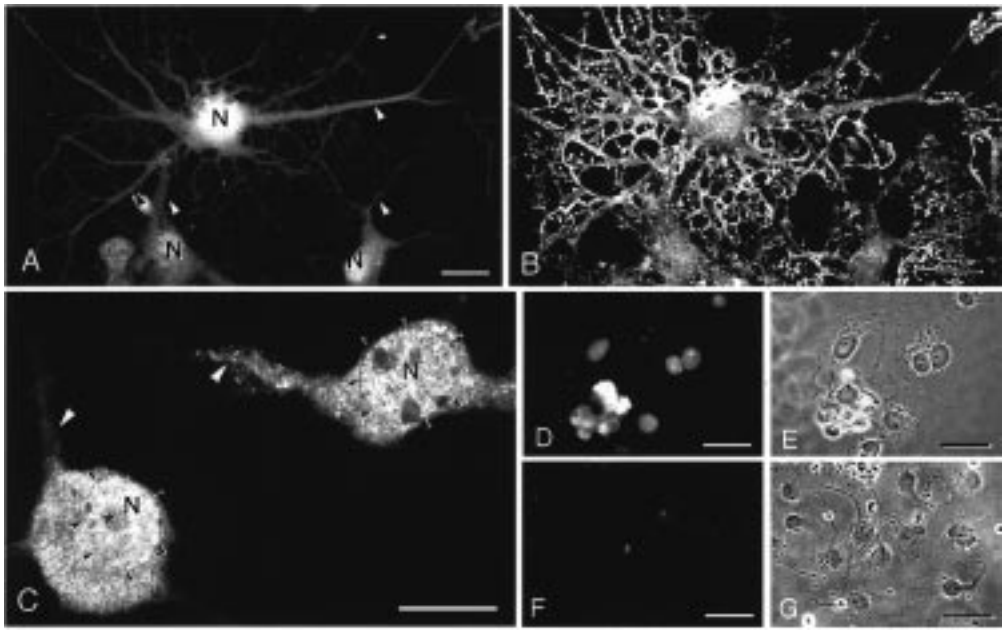

FIGURE 6: hnRNP A2 distribution in tissue cultures of mouse oligodendrocytes (A−C) and COS-1 cells (D−G). (A) Confocal microscope images of hnRNP A2 (HK334-8 antibody) immunofluorescence demonstrate staining of oligodendrocyte nuclei (N; three oligodendrocytes in this field) and in the major cytoplasmic processes (arrowheads) radiating from the cell somata. (B) Immunolabeling for MBP in the same cells highlights areas of myelin membrane expansion. (C) Higher magnification imaging through two oligodendrocyte cell bodies demonstrates the granular pattern of hnRNP A2 immunostaining in both nuclear (N; small arrowheads mark the nuclear envelope) and cytoplasmic compartments. hnRNP-containing granules extended into the major cytoplasmic processes (arrowheads), which continue beyond this focal plane. Within nuclei, hnRNP A2 is characteristically excluded from nucleoli (asterisk). (D, E) In COS-1 cells, hnRNP A2 immunostaining labels principally the nucleus, while in control cultures (F, G), omission of the HK334-8 antibody produces no specific staining when photographed under identical lighting and image-capture conditions (panels D and F, epifluorescence micrographs; panels E and G, phase-contrast images of the same cells). Scale bars for panels A−C are 10 μm; for panels D−G, 25 μm.

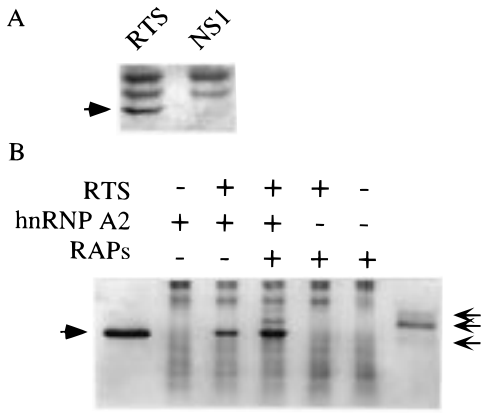

FIGURE 7: RTS-binding characteristics of isolated hnRNP A2 and RAPs. (A) HPLC-purified rat brain hnRNP A2 was incubated with magnetic particles labeled with RTS RNA (left lane) or nonspecific RNA (NS1, right lane), with 5 g/L BSA and 10 g/L heparin added to inhibit nonspecific binding to the particles. The bound proteins were eluted and run on an SDS−polyacrylamide gel, which was stained with silver. hnRNP A2 (arrow) binds the RTS in the absence of other RTS-associated polypeptides but does not bind NS1. The top two bands are derived from the added BSA. (B) RTS-binding characteristics of isolated RAPs. HPLC-purified proteins were incubated with magnetic particles that were either labeled with RTS RNA (+) or unlabeled (−), with 5 g/L BSA added to inhibit nonspecific binding to the particles. The bound proteins were eluted and run on an SDS−polyacrylamide gel, which was stained with B/T Bl*v* protein stain. hnRNP A2 (large arrow, left lane) binds the RTS in the absence of other RTS-associated polypeptides (small arrow, right lane), but other RAPs do not bind RTS in the absence of hnRNP A2.

to MBP mRNA, these granules also contain other mRNAs and probably much of the apparatus required for translation. Translation appears unnecessary for translocation, as MBP RNA constructs lacking the coding region are still transported efficiently (*18*).

hnRNPs as trans-Acting Factors. Most *trans*-acting factors implicated in RNA localization or translational activation have been identified only as bands on autoradiographs of gel mobility shift assays. Some of the better characterized, such as Spnr, a 71-kDa protein expressed at high levels in brain, ovary, and testis that is involved in RNA transport or translational activation, show little sequence similarity with hnRNPs (*37*). But several hnRNPs or hnRNP-like proteins have been implicated in these aspects of cytoplasmic RNA metabolism. Stabilization elements in the 3′-UTR of precursor amyloid protein mRNA are recognized by C-type hnRNPs (*38*). hnRNPs K and E1 silence the translation of rabbit erythroid 15-lipoxygenase (*39*). FBP (far upstream element binding protein), which shares some peptide sequences with hnRNP K, binds to a 26-nt stabilization element of the 3′-UTR of GAP-43, a neuronal protein (*33*). ZBP-1, a 68-kDa protein with structural similarity to hnRNPs that possess RNP sequences, binds to the β-actin mRNA localization "zip code" (*40*).

The hnRNPs are a family of over 20 RNA-binding proteins, many of which are characterized by the presence of one or more RNA-binding domain motifs (*41*, *42*). In the HeLa cell nucleus, the core hnRNPs (A1, A2, B1, B2, C1, and C2) assemble onto hnRNAs in a sequence-independent manner, binding cooperatively and with fixed stoichiometry to package ~700-nt hnRNA segments into 40S particles (*43*, *44*). However, hnRNPs also recognize discrete target sequences within several RNAs and DNAs (*37*, *45*, *46*). hnRNPs of the A, B, C, D, and I families recognize polypyrimidine-rich splice-site sequences (*47*, *48*). hnRNP

A2 also binds telomeric DNA and RNA sequences (*49*). The RTS contains no polypyrimidine-rich sequences, such as splice-site, rapid turnover, or telomere-like motifs, nor any other target sequence so far identified for other RNA-binding proteins. Our experiments thus indicate that MBP mRNA's *cis*-element, the RTS, is selectively recognized by hnRNP A2.

Is hnRNP A2 part of a *trans*-acting translocation factor? The nonspecific association of this protein with hnRNA is well documented, but the association with the RTS appears fundamentally different. We appear not to have simply isolated nuclear core particles in our experiments; the core particles that have been described for HeLa cells have the composition (3A1:1B2:3A2:1B1:3C1:1C2), whereas hnRNP A2 is clearly the dominant RTS-binding protein. As the RTS is a small RNA segment with a demonstrated role in the cytoplasmic transport of MBP mRNA, the association of the hnRNP A2 with this element suggests its participation in this process.

Cytoplasmic Roles for hnRNPs. These results add to the growing body of research (*20, 38, 50*) indicating that some hnRNPs may serve important functions outside the nucleus. Our demonstration that hnRNP A2 is present in distal myelinating processes of oligodendrocytes reinforces the view that this protein not only may shuttle between nucleus and cytoplasm but also remains associated with some cytoplasmic mRNAs and may contribute to their metabolism. The observation that nuclear RNA-binding proteins such as hnRNP A1, hnRNP A2 (*20*), hnRNP C (*38*), and hrp40 (*50*) may shuttle between the nucleus and cytoplasm, and influence RNA processing in both compartments, adds an important new layer of complexity to the posttranscriptional regulation of protein synthesis.

RTS-Associated Proteins. The five RAPs are far less abundant than hnRNP A2 in the protein fraction recovered from the RTS-labeled magnetic beads, and initial attempts to obtain their amino acid sequences by Edman degradation have not succeeded. Western blots developed with the 7A9 antibody suggest that two of the RAPs may be other hnRNPs, but the HPLC-purified group of proteins shows little affinity for the RTS in the absence of A2 (Figure 7B), and confirmation of their identity is required.

If these proteins form a single particle with hnRNP A2, the SDS gel staining and the relative sizes of the reverse-phase HPLC peaks lead to the conclusion that there must be several copies of the hnRNP A2 in the complex. There is an interesting parallel between this putative complex of hnRNP A2 with the RAPs and dynactin, the latter combining multiple copies of the actin-related protein, Arp1, and single copies of several other polypeptides (*51, 52*).

In a recent paper, mouse translin was identified as a factor, concentrated in brain and testis, that binds an RTS-like sequence (the H-element) in the protamine 2 mRNA 3′-UTR (*53*). This 26.2-kDa DNA recombination protein, which is associated with chromosomal translocations, also recognizes a 284-nt segment of the MBP mRNA 3′-UTR, which includes the RTS (*54*). In our assays using testis or brain extracts, even under conditions of protein overloading, this protein was not detected among those preferentially bound to the RTS. None of the concensus binding sequences for translin (*55*) are present within the RTS.

A Common Mechanism for RNA Transport? mRNA localization contributes to the morphological polarization of many important cells (*1, 32*), and at least some of the mechanisms responsible to be appear conserved, even across widely disparate species (*56*). The high cytoplasmic concentration of hnRNP A2 in some tissues, including brain and testis (*57*; this study), suggests that it may be involved with mRNA-related processes other than intranuclear RNA processing and transport. This *trans*-acting factor may also bind to more than MBP mRNA, as recent surveys of the sequence databases (*18, 54*) have indicated RTS-like motifs in a number of mRNAs, including MAP2A, neurogranin, and glial fibrillary acidic protein (*18*).

ACKNOWLEDGMENT

We thank Dr. Gideon Dreyfuss, University of Pennsylvania, for providing us with the 7A9 monoclonal antibody, and Amanda Hawkins, University of Queensland, for assistance in generating the chicken antibody to hnRNP A2.

REFERENCES

1. St. Johnston, D. (1995) *Cell 81*, 161−170.
2. Pokrywka, N. J. (1996) *Curr. Top. Dev. Biol. 31*, 139−166.
3. Kislauskis, E. H., Li, Z., Singer, R. H., and Taneja, K. L. (1993) *J. Cell Biol. 123*, 165−172.
4. Kleiman, R., Banker, G., and Steward, O. (1994) *J. Neurosci. 14*, 1130−1140.
5. Behar, L., Marx, R., Sadot, E., Barg, J., and Ginzburg, I. (1995) *Int. J. Dev. Neurosci. 13*, 113−127.
6. Colman, D. R., Kreibich, G., Frey, A. B., and Sabatini, D. D. (1982) *J. Cell Biol. 95*, 598−608.
7. Trapp, B. D., Moench, T., Pulley, M., Barbosa, E., Tennekoon, G., and Griffin, J. (1987) *Proc. Natl. Acad. Sci. U.S.A. 84*, 7773−7777.
8. Stoffel, W. (1990) *Angew. Chem., Int. Ed. Engl. 29*, 953−976.
9. Moscarello, M. A. (1990) in *Dynamic Interactions of Myelin Proteins* (Hashim, G. A., and Moscarello, M. A., Eds.) pp 25−48, Alan R. Liss Inc., New York.
10. Smith, R. (1992) *J. Neurochem. 59*, 1589−1608.
11. Readhead, C., Popko, B., Takahashi, N., Shine, H. D., Saavedra, R. A., Sidman, R. L., and Hood, L. (1987) *Cell 48*, 703−712.
12. Brophy, P. J., Boccaccio, G. L., and Colman, D. R. (1993) *Trends Neurosci. 16*, 515−521.
13. Sorg, B. A., Smith, M. M.,, and Campagnoni, A. T. (1987) *J. Neurochem. 49*, 1146−1154.
14. LoPresti, P., Szuchet, S., Papasozomenos, S. C., Zinkowski, R. P., and Binder, L. I. (1995) *Proc. Natl. Acad. Sci. U.S.A. 92*, 10369−10373.
15. Ainger, K., Avossa, D., Morgan, F., Hill, S. J., Barry, C., Barbarese, E., and Carson, J. H. (1993) *J. Cell Biol. 123*, 431−441.
16. Amur-Umarjee, S., Phan, T., and Campagnoni, A. T. (1993) *J. Neurosci. Res. 36*, 99−110.
17. Barbarese, E., Koppel, D. E., Deutscher, M. P., Smith, C. L., Ainger, K., Morgan, F., and Carson, J. H. (1995) *J. Cell Sci. 108*, 2781−2790.
18. Ainger, K., Avossa, D., Diana, A. S., Barry, C., Barbarese, E., and Carson, J. H. (1997) *J. Cell Biol. 138*, 1077−1087.
19. Enan, E., and Matsumara, F. (1995) *Biochem. Pharmacol. 49*, 249−261.
20. Piñol-Roma, S., and Dreyfuss, G. (1992) *Nature 355*, 730−732.
21. Piñol-Roma, S., and Dreyfuss, G. (1991) *Science 253*, 312−314.
22. Burd, C. G., Swanson, M. S., Görlach, M., and Dreyfuss, G. (1989) *Proc. Natl. Acad. Sci. U.S.A. 86*, 9788−9792.

23. Riva, S., Morandi, C., Tsoulfas, P., Pandolfo, M., Biamonti, G., Merrill, B., Williams, K. R., Multhaup, G., Beyreuther, K., Werr, H., Henrich, B., and Schäfer, K. P. (1986) *EMBO J. 5*, 2267−2273.
24. Cobianchi, F., Biamonti, G., Maconi, M., and Riva, S. (1994) *Genetica 94*, 101−114.
25. Birney, E., Kumar, S., and Krainer, A. R. (1993) *Nucleic Acids Res. 21*, 5803−5816.
26. Idriss, H., Kumar, A., Casas-Finet, J. R., Guo, H., Damuni, Z., and Wilson, S. H. (1994) *Biochemistry 33*, 11382−11390.
27. Rajpurohit, R., Paik, W. K., and Kim, S. (1994) *Biochem. J. 304*, 903−909.
28. Faura, M., Renau-Piqueras, J., Bachs, O., and Bosser, R. (1995) *Biochem. Biophys. Res. Commun. 217*, 554−560.
29. Hesketh, J. E., and Pryme, I. F. (1991) *Biochem. J. 277*, 110.
30. Kim-Ha, J., Webster, P. J., Smith, J. L., and Macdonald, P. M. (1993) *Development 119*, 169−178.
31. Singer, R. (1993) *Curr. Biol. 3*, 719−721.
32. Bassell, G., and Singer, R. H. (1997) *Curr. Opin. Cell Biol. 9*, 109−115.
33. Irwin, N., Baekelandt, V., Goritchenko, L., and Benowitz, L. I. (1997) *Nucleic Acids Res. 25*, 1281−1288.
34. Gavis, E. R., Curtis, D., and Lehmann, R. (1996) *Dev. Biol. 176*, 36−50.
35. Holcik, M., and Liebhaber, S. A. (1997) *Proc. Natl. Acad. Sci. U.S.A. 94*, 2410−2414.
36. Carson, J. H., Worboys, K., Ainger, K., and Barbarese, E. (1997) *Cell Motil. Cytoskel. 38*, 318−326.
37. Schumacher, J. M., Lee, K., Edelhof, S., and Braun, R. E. (1995) *J. Cell Biol. 129*, 1023−1032.
38. Zaidi, S. H. E., and Malter, J. S. (1995) *J. Biol. Chem. 270*, 17292−17298.
39. Ostareck, D. H., Ostareck-Lederer, A., Wilm, M., Thiele, B. J., Mann, M., and Hentze, M. W. (1997) *Cell 89*, 597−606.
40. Ross, A. F., Oleynikov, Y., Kislauskis, E. H., Taneja, K. L., and Singer, R. H. (1997) *Mol. Cell. Biol. 17*, 2158−2165.
41. Dreyfuss, G., Matunis, M. J., Piñol-Roma, S., and Burd, C. G. (1993) *Annu. Rev. Biochem. 62*, 289−321.
42. Mattaj, I. W. (1993) *Cell 73*, 837−840.
43. Schenkel, J., Sekeris, C. E., Alonso, A., and Bautz, E. K. F. (1988) *Eur. J. Biochem. 171*, 565−569.
44. Barnett, S. F., Theiry, T. A., and LeStourgeon, W. M. (1991) *Mol. Cell. Biol. 11*, 864−871.
45. Burd, C. G., and Dreyfuss, G. (1994) *EMBO J. 13*, 1197−1204.
46. Görlach, M., Burd, C. G., and Dreyfuss, G. (1994) *J. Biol. Chem. 269*, 23074−23078.
47. Swanson, M. S., and Dreyfuss, G. (1988) *EMBO J. 7*, 3519−3529.
48. Mayeda, A., and Krainer, A. R. (1992) *Cell 68*, 365−375.
49. McKay, S. J., and Cooke, H. (1992) *Nucleic Acids Res. 20*, 6461−6464.
50. Matunis, E. L., Kelley, R., and Dreyfuss, G. (1994) *Proc. Natl. Acad. Sci. U.S.A. 91*, 2781−2784.
51. Allan, V. (1994) *Current Biol. 4*, 1000−1002.
52. Schafer, D. A., Gill, S. R., Cooper, J. A., Heuser, J. E., and Schroer, T. A. (1994) *J. Cell Biol. 126*, 403−412.
53. Wu, X.-Q., Gu, W., Meng, X., and Hecht, N. B. (1997) *Proc. Natl. Acad. Sci. U.S.A. 94*, 5640−5645.
54. Han, J. R., Gu, W., and Hecht, N. B. (1995) *Biol. Reprod. 53*, 707−717.
55. Aoki, K., Suzuki, K., Sugano, T., Tasaka, T., Nakahara, K., Kuge, O., Omori, A., and Kasai, M. (1995) *Nat. Genet. 10*, 167−174.
56. Litman, P., Behar, L., Elisha, Z., Yisraeli, J. K., and Ginzburg, I. (1996) *Dev. Biol. 176*, 86−94.
57. Kamma, H., Portman, D. S., and Dreyfuss, G. (1995) *Exp. Cell Res. 221*, 187−196.

BI9800247